Using SWAT Model to Assess the Impacts of Land Use and Climate Changes on Flood in the Upper Weihe River, China

Yinge Liu [1], Yuxia Xu [1,*], Yaqian Zhao [2,3] and Yan Long [1]

[1] Key Laboratory of Disaster Monitoring and Mechanism Simulating of Shaanxi Province, Baoji University of Arts and Sciences, Baoji 721013, China; liuyinge@bjwlxy.edu.cn (Y.L.); dragonfacely@163.com (Y.L.)
[2] Department of Municipal and Environmental Engineering, School of Water Resources and Hydro-Electric Engineering, Xi'an University of Technology, Xi'an 710048, China; yzhao@xaut.edu.cn
[3] Dooge Centre for Water Resources Research, School of Civil Engineering, University College Dublin, D04 V1W8 Dublin 4, Ireland
* Correspondence: xuyuxia@bjwlxy.edu.cn

Abstract: Flood disasters have occurred frequently in recent years, but there is no consensus on the mechanism and influencing factors. Taking the upper reaches of Weihe River Basin as a case in Western China, a soil and water assessment tool (SWAT) model was established to quantitatively simulate the impact of land use and climate change on runoff changes, while 4 extreme land-use scenarios and 24 temperature and precipitation scenarios assumptions were proposed to simulate the response of runoff to land use and climate changes. The SWAT simulation results showed that the sensitivity parameters affecting the model simulation were the CANMX, CN2, SOL_K, CH_N2, and SOL_AWC. The correlation index R^2 and the efficiency coefficient E_{NS} of the upper Weihe River were both in the range of 0.75–0.78, the relative error PS between the simulated results and the measured runoff was below 10%, suggesting the good applicability of the SWAT model in this study area. Using the improved SWAT model to simulate the peak runoff (flood) simulation value is generally smaller than the measured value, and the absolute value of the error is less than 6%. The expansion of wasteland increased the runoff by over 90% on average, the expansion of cultivated land increased the runoff by 8% on average, and the expansion of woodland and grassland increased the surface runoff by 6% on average. When the precipitation decreased by 25% and the temperature increased by 22%, the smallest runoff was obtained in the simulation. Accordingly, when the precipitation increased by 25% and the temperature decreased by 22%, the maximum annual runoff was obtained. By decomposing the contribution rate of human activities and climate change to runoff, it showed that the contribution rate of human activities to the reduction of runoff was greater than that of climate change. This study can provide scientific reference for the simulation and prediction of future floods.

Keywords: upper Weihe River; SWAT model; hydrological runoff; land use; climate change

1. Introduction

Flood is a natural disaster. With global warming, which human activity accelerates, the frequency, intensity, and impact of floods are gradually increasing, which have seriously threatened agriculture, industry, transportation, and lifeline projects, causing huge economic losses in countries worldwide, such as China, the United States, France, Bangladesh, Nepal, Bhutan, and Sri Lanka [1–3]. Therefore, the assessment of flood changes is becoming more important. The impact of climate and land use changes on the hydrology and water resources of basins is an important basis for adaptive watershed management [4,5]. It is also very urgent to assess the impact of climate change, especially precipitation change, on water resources and the water cycle [6,7]. Compared with the long-term characteristics of climate change, land use and cover change is one of the main driving factors of hydrological changes in the basin in a short term [7,8]. It affects the hydrological cycle of the basin by

affecting canopy interception, surface infiltration, evapotranspiration, and surface runoff. Therefore, the study of climate change and land use on the hydrological cycle and floods has become a focus of attention.

In order to develop flood forecasts with clearer physical mechanisms, it is necessary to continuously deepen the understanding of the hydrological laws of the basin. The formation process of runoff in nature is a complex process under the interaction of many factors. Although it has a certain randomness, regularities can be found from it [9] For example, the variable infiltration capacity model (VIC) was used to simulate the energy balance and water balance in the process of water cycle at the same time. Environmental policy integrated climate model (EPIC) was employed to quantitatively assess the integrated dynamics of the climate-soil-crop-management system. Gridded surface and groundwater hydrological analysis model (GSSHA) was adopted to analyze and simulate surface runoff and groundwater. A Distributed hydrological soil vegetation Model (DHSVM) was used to simulate the hydrological process of a watershed at a high spatial and temporal resolution. A Water Erosion Prediction Project Model (WEPP) was used to predict soil erosion and sediment transport day by day. An Annual Agricultural Non-Point Source Pollution Model (AnnAGNPS) was able to simulate water, sand, transport and hydrological processes. A European hydrological system model (Mike-SHE) was a comprehensive, deterministic and physically meaningful distributed hydrological system model for simulating almost all hydrological processes [10,11]. These models have improved the prediction accuracy, but the research on its mechanism is still lacking, especially the research on the response mechanism of the hydrological cycle under climate change has become a major problem.

In particular, the SWAT model was widely used for watershed simulation under different land management conditions, soil types and land use patterns. For example, Pongpetch et al. [12] used the SWAT model to simulate the flow and sediment of the Lam Takong River Basin in Thailand and evaluated the regional sediment and nutrient load. Jung et al. [13] applied the SWAT hydrological model and Budyko curve to assess the impact of potential CO_2 changes on the hydrological cycle of the forest-dominated Seolma-cheon watershed in Korea. Golmohammadi et al. [14] used the SWAT hydrological model to simulate and predict runoff-generating areas in the Gully Creek watershed in Ontario, Canada, which provided a reference for runoff generation modeling in the basin. Lucas-Borja et al. [15] used the SWAT model to simulate and predict runoff in a small watershed in the tropical forest of Brazil. They believed that the watershed runoff has a decreasing trend. Amin et al. [16] simulated the runoff of the Mojo River in the Yes, it's Korea.

Upper reaches of the Awash River in Ethiopia based on the SWAT model, verifying the consistency between the simulation results and the measured values. Shrestha et al. [17] used the SWAT model to analyze the relationship between climate, flow, and sediment production in the Swat River Basin in Pakistan, which suggested that developing a sedimentary basin was the most economical option for soil erosion mitigation management under climate change. A number of studies [18–22] adopted the SWAT hydrological model to analyze the impact of climate and human factors on runoff, believing that the influence of climate was decreasing, while the influence of man-made influence was increasing. It can be seen from the above studies that although the SWAT model has been used to study the influencing factors of runoff in small watersheds, the core elements affecting runoff and flood patterns have not been comprehensively understood from the aspects of land use and climate change. Other methods have also been applied to quantitatively analyze the impact of climate and land use changes on the river basin runoff, such as comparative watershed experiment, statistical analysis, and model simulation [23], as well as the Mann–Kendall trend test method, Budyko water and heat balance equation calculation method, regional climate model (RCM) and other methods [24]. For example, Ning et al. [24] used a Mann–Kendall trend test and Budyko water-heat balance equation to analyze the effects of climate change and human activities on runoff changes in four typical river basins in China. Jha et al. [25] evaluate the impact of climate change on stream flow in the Upper

Mississippi River Basin (UMRB) by using a regional climate model (RCM) coupled with a hydrologic model, SWAT, suggesting that a 21% increase in future precipitation simulated by the RCM produced an 18% increase in snowfall and a 51% increase in surface runoff. Other approaches were used to study some world's large rivers basins and showed that changes in runoff of most rivers in North Asia and Northern Europe were significantly affected by rainfall [26–30].

It has been noted that the above studies have given some consideration to the impact of the temporal and spatial variability of climate, topography, soil, vegetation, etc. on the runoff. However, the research was lack of impact mechanism of extreme hydrological events on climate change and human activities in different climatic environments, land surface processes. Climate change and strong human activities (such as water conservancy project construction, reservoir regulation and storage, etc.) have affected extreme weather and climate events [3]. In the future, the impact of human activities on extreme hydrological events should be further considered, especially the quantitative separation of natural climate variability, anthropogenic climate change and the impact mechanism of human activities on the hydrology of the underlying surface, which will seriously threaten the national flood control security, water supply security, food security, and ecological environment security.

Flood is an extreme reflection of runoff changes. In recent years, the frequency of floods has increased year by year. The main defense of floods is prevention rather than control, so the research on defense is of great significance. For example, Yazdani et al. [1] and Ishiwatari et al. [2] conducted flood disaster risk and an empirical analysis on the relationship between investment and damage in major flood-prone countries in Asia using multiple regression models to analyze The relationship between flood protection investment and flood damage and other socioeconomic development. Shreevastav et al. [3] objectively assessed the vulnerability of community life in the upper, middle, and lower reaches of the Bagmati River corridor in southern Nepal; using data obtained from questionnaires and interviews, the Livelihood Vulnerability Index (LVI and IPCC-LVI) was calculated in conjunction with the IPCC definition and the Sustainable Livelihoods Framework. Hagen et al. [31] advocate a stronger interface between model developers and model users to develop flood forecasting models based on forecast financing to support global disaster reduction risk escalation. The above research can help to support the planning and construction of flood hazard risk minimization and flood shelters of local government, and even for national and international level. These studies provide some good approaches for flood prevention, but there is still a lack of research on the prevention mechanism, especially the research on the mechanism of flood occurrence.

Although the above studies have achieved fruitful results in flood prevention, there were few studies on the simulation of flood influencing factors and the mechanism. In order to meet the above challenges, it is crucial to strengthen the scientific research on the response mechanism of the hydrological cycle under climate change. However, how to quantitatively separate the contributions of climate change and human activities to the evolution of extreme runoff has become a difficult problem.

Therefore, in this paper, the Weihe River Basin was selected for case study, which is located in the Loess Plateau region of western China with the intensification of human activities and climate change. Through parameter analysis and calibration, small watershed units were divided, while the model to improve watershed flood simulation and prediction was established. Through basin hydrological simulation and future runoff prediction, the impact mechanism was then discussed, which is associated with natural climate variability, anthropogenic climate change and human activities on the underlying surface on hydrology. Compared with the runoff process, the flood process has the characteristics of short time, high intensity and fast runoff, which requires a more refined model to simulate. Therefore, we attempted to divide fine watershed units through parameter analysis and calibration and establish an improved model for flood simulation and prediction of watershed. Meanwhile, simulation of the impact of land use and climate change on floods was conducted based

on scenario assumptions. Thus, it will help to analyze the influence mechanism of human activities on floods. The research outcome can provide scientific reference for the simulation and prediction of future floods and disaster prevention.

2. Materials and Methods

2.1. Study Area

The upper reach of the Weihe River is located between $33°43'$ N–$36°10'$ N and $103°31'$ E–$107°30'$ E with the length of about 410 km, as shown in Figure 1. The catchment area is about 40,000 km^2 with many mountains, undulating terrains and a continental monsoon climate. The average annual rainfall is about 540 mm, while the annual average runoff is about 2.2×108 m^3 with large inter-annual changes, frequent flooding in the basin, with a maximum peak flow of 5030 m^3·s^{-1} (on 17 August 1954). The changes in river runoff have a greater response to reflecting climate and land use changes. Floods often occur in summer and autumn. Therefore, it is of great significance to study the runoff changes in the Weihe River Basin.
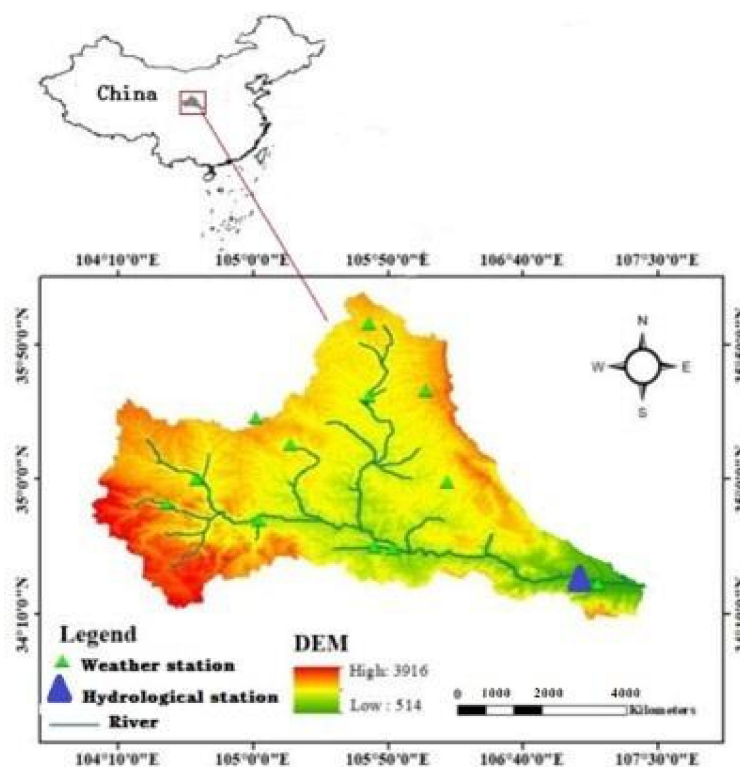
Figure 1. Location of the study area.

2.2. Construction of Basic Database

In this study, the SWAT model was used to simulate and analyze the impact of climate change and human activities on flood flow, which required two basic data sets, i.e., geospatial data and attribute data. The former included DEM, land use type, and soil type, while the latter included soil database, land use database, and meteorological and hydrological database. The data sets were constructed as follows:

(1) Spatial data: ArcGIS was used to splice, project transformation, fill depressions, analyze flow direction, and extract watersheds from the original DEM data (30 m × 30 m) to obtain a digital elevation model of the upper Weihe River. The data were sourced from the geospatial data cloud network (http://www.gscloud.cn, accessed on 9 September 2020).

(2) Soil database: The soil database included soil type data and soil attribute data. After loading the original soil type data in ArcGIS18.0 software (Esri Corporation, Redlands, CA, USA) with resolution of 50 m × 50 m, operations such as projection, clipping,

and reclassification were performed to obtain the soil type map of the study area (Figure 2a). The soil attribute database was sourced from the Cold and Arid Regions Science Data Center (http//westdc.westgis.ac.cn, accessed on 19 September 2020). There were a total of 19 soil types (see Figure 2b) in the upper Weihe River, including Calcaric Cambisols CMc, Gleyic Luvisols LVg, Dystric Cambisols CMd, Haplic Luvisols LVh, CumulicAnthrosols ATc, Eutric Cambisols CMe, Calcic Luvisols LVk, FimicAnthrosols ATf, Gleyic Cambisols CMg, Gleyic Phaeozems PHg, Haplic Chernozems CHh, CalcaricFluvisols FLc, Haplic Phaeozems PHh, Calcic Chemozems CHk, Haplic Greyzems GRh, CalcaricRegosols RGc, Luvic Chernozems CHl, Albic Luvsiols LVa, and Eutric Regosols RGe.

(3) Land use database: The land use database used in this article was a two-level classification system developed by the Chinese Academy of Sciences with resolution of 50 m × 50 m. The land use types of the study area were divided into eight types, i.e., cultivated land, woodland, grassland, water area, residential area, residential area (low density), transportation land, wasteland, and bare land (Figure 2b). The data were sourced from the Cold and Arid Regions Science Data Center (http//westdc.westgis.ac.cn, accessed on 11 September 2020).

(4) Weather database. The meteorological data required by the SWAT model included daily data of precipitation, maximum temperature, minimum temperature, relative humidity, wind speed, and solar radiation. The solar radiation data were obtained from the weather generator. The daily precipitation, maximum and minimum temperature from the National Information Center during 1960 to 2019 were actual measurements. Other required meteorological data were generated using weather software to assist in calculation. The data were sourced from China Meteorological Data Network (http://data.cma.cn, accessed on 21 September 2020).

(5) Hydrological database: The hydrological data of 1975–2019 used in the paper was from Linjiacun Hydrological Station. Because Linjiacun Hydrological Station governs all the runoff in the upper reaches of the Weihe River and was the outlet of the entire upper reaches, the runoff of Linjiacun Hydrological Station was used to represent the runoff in the upper Weihe River.
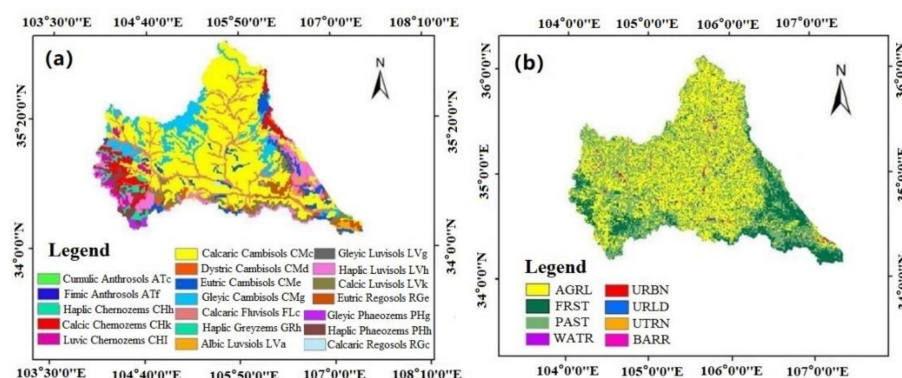
Figure 2. Distribution of soil types (**a**) and land cover types (**b**).

2.3. Methods

2.3.1. SWAT Model

The main elements reflecting floods included runoff, flood peaks, and precipitation. SWAT can well simulate regional runoff changes. Therefore, it was used to assess the impact of climate change and human activities on floods. SWAT model was composed of the hydrological cycle runoff process, the slope confluence land process, and the river confluence process [32]. The surface hydrological process in this study was mainly divided into the land the hydrological cycle and the river confluence process. In the land hydrological cycle, the simulation was mainly based on the water balance equation, as shown in Equation (1):

$$SW_t = SW_0 + \sum_{i=1}^{t}\left(R_{day} - Q_{surf} - E_a - W_{seep} - Q_{gw}\right) \tag{1}$$

where, SW_t was the final soil moisture content, SW_0 was the early soil moisture content (mm), t was the time step (day), R_{day} was the i-th rainfall (day), Q_{surf} was the i-th day surface runoff (mm), E_a was the i-th day evaporation (mm), W_{seep} was the infiltration and lateral flow at the bottom of the soil profile on the i-th day (mm), and Q_{gw} was the groundwater outflow on the i-th day (mm).

The calculation in river confluence was divided into main river calculation and reservoir calculation. The main river calculation included the water flow, sediment, nutrients, and organic chemical substances, while the reservoir calculation included the inflow, outflow, surface precipitation, evaporation, leakage at the bottom of the reservoir, diversion and return flow, etc. The variable storage model and the Muskingum method were utilized in the calculation, as shown in Equation (2):

$$q_{out,2} = q_{out,1} + SC \cdot q_{in,ave} - SC \cdot q_{out,1} \tag{2}$$

where, $q_{out,1}$ and $q_{out,2}$ were the change rates of outflow at the beginning and end of the time step (m^3/s), respectively, $q_{in,ave}$ represented the average outflow rate of runoff from the river within the time step, and SC represented the storage coefficient.

2.3.2. Division of Sub-Basin

The division of tributaries played an important role in model construction and simulation verification. Firstly, by filling the topographic data to reduce the topographic error caused by different landforms, and then, the hydrological response unit (HRUs) was determined. Each sub-watershed was divided into several hydrological response units (HRUs) according to the underlying surface characteristics such as land use, soil, and slope. For sub-watershed division, the smaller the design threshold of ponding area was, the finer the unit division, and the denser the grid was, the higher the simulation accuracy. Regarding the actual situation of the study area and considering the calculation speed of the model, the minimum catchment area threshold was set to 500 km^2, and the slope of the study area was divided into two grades of 0~5° and above 5°. Soil type, land use, and slope account for 10%, 10%, and 15% of the sub-watershed area, respectively. Finally, the upper Weihe River Basin was divided into 43 sub-basins, and 315 hydrological response units (HRU), as shown in Figure 3.
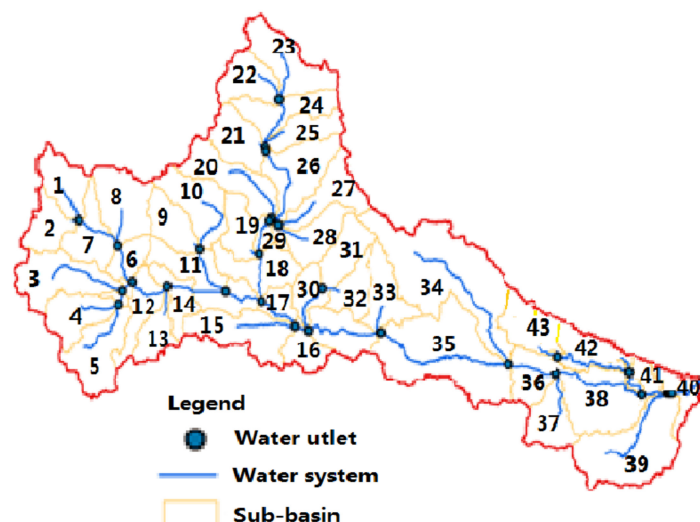

Figure 3. Sub-basin division of upper Weihe River.

2.3.3. Evaluation of Model

In order to reduce the blindness of calibration parameters and improve the efficiency of model operation and the accuracy of simulation results, it was necessary to conduct evaluation on simulation results of SWAT. In this paper three indicators, i.e., the commonly used certainty coefficient (R^2), Nash-Sutcliffe coefficient (NSE), and PBIAS, were selected to evaluate the quality of the model simulation results.

The calculation formulas of ENS, R^2 and PBIAS were expressed as Equations (3)–(5), respectively:

$$E_{NS} = 1 - \sum_{i=1}^{n}(Q_{obs} - Q_{sim})^2 / \sum_{i=1}^{n}(Q_{obs} - Q_{assim})^2 \tag{3}$$

$$R^2 = \sum_{i=1}^{n}[(Q_{sim} - Q_{asim})(Q_{obs} - Q_{aobs})]^2 / \sum_{i=1}^{n}(Q_{sim} - Q_{asim})^2 \sum_{i=1}^{n}(Q_{obs} - Q_{aobs})^2 \tag{4}$$

$$PBLAS = \frac{\sum_{i=1}^{n}(Q_{obs} - Q_{sim})}{\sum_{i=1}^{n} Q_{obs}} \times 100\% \tag{5}$$

where, Q_{sim} refers to the simulated runoff value, Q_{obs} represents the measured runoff, Q_{asim} and Q_{aobs} represent the average values of the simulated runoff and the measured runoff, respectively. E_{NS} was used to verify the performance of the hydrological model simulation results. The closer the E_{NS} was to 1, the more consistent the simulated value was with the measured value, and the more accurate the simulation result [33]. When $E_{NS} < 0.54$, the simulation result was acceptable; when $0.54 \leq E_{NS} \leq 0.65$, the simulation result was more satisfactory; and when $E_{NS} > 0.65$, the simulation result was very good. R^2 represented the goodness of fit between the simulated runoff value and the measured value. The closer R^2 was to 1, the better the fit between the simulated value and the measured value. When $R^2 = 1$, the simulated value was in complete agreement with the measured value. It was generally considered that when $R^2 > 0.6$, the simulation results were relatively satisfactory. The ratio of the simulated runoff value to the measured value was defined as the relative error PBIAS, which can reflect the credibility of the simulation results. When PBIAS > 0, the simulated value was too small; when PBIAS < 0, the simulated value was too large; when $15 < |PBIAS| < 25$, the simulation result was acceptable; when $10 < |PBIAS| < 15$, the simulation result was good; and when $|PBIAS| < 10$, the simulation result was very good.

In addition, *p* factor and r factor were used for evaluation of model performance. The *p* factor represented the proportion of data enclosed by the 95PPu band, while the r factor represented the mean width of the 95PPu band and the standard deviation of the measured variable [34–36].

2.3.4. Cumulative Slope Change Rate Comparison Method

In this paper, we choose a cumulative slope change rate comparison approach to decompose the contribution of climate change and land use to floods, and the contribution rate of climate change to runoff mainly included the impact of precipitation change on runoff and the impact of potential evapotranspiration on runoff.

The contribution rate of precipitation to runoff can be described as follows. Assuming that the slopes of the linear relationship between cumulative runoff and the year were S_{Rb} and S_{Ra} in the two periods before and after the inflection point, respectively, while the slopes of the precipitation in the two periods before and after the inflection point were S_{Pb} and S_{Pa}, respectively, the cumulative runoff slope change rate was $[(S_{Ra} - S_{Rb})/|S_{Rc}|]$. Similarly, the cumulative precipitation slope change rate was $[(S_{Pa} - S_{Pb})/|S_{Pc}|]$, then the contribution rate C_P of precipitation to the change of runoff was

$$C_P = [(S_{Pa} - S_{Pb})/|S_{Pb}|]/[(S_{Ra} - S_{Rb})/|S_{Rb}|] \times 100\% \tag{6}$$

In the same way, the contribution rate C_E of potential evaporation to the change of runoff can also be calculated to further estimate the contribution rate of climate change to the decrease in the runoff.

On this basis, the contribution rate C_H of human activities to the change of runoff can be calculated as

$$C_H = 1 - C_P - C_E \tag{7}$$

2.4. Land Use and Climate Scenarios

2.4.1. Land Use Scenario Assumptions

In order to further analyze the impact of specific land use type changes on runoff, this paper simulated the regional annual and monthly runoff by establishing land use scenarios. Generally, land use scenario analysis methods included the reference comparison method, historical inversion method, model prediction method, extreme scenario hypothesis method, spatial allocation method, etc. [37]. We selected the extreme land use scenario hypothesis method, i.e., all one or more land use types were converted to another land use type, as shown in Table 1, four extreme land use scenarios were assumed, namely:

(1) Scenario 1 (LU-S1): Based on the policy of returning farmland to forest, it was assumed that all cultivated land and wasteland were converted into forest land. The land use types of the upper reaches of the Weihe River in this scenario were forest land, grassland, water area, residential area, and traffic land.

(2) Scenario 2 (LU-S2): Based on the policies such as returning farmland to grassland and rational grazing, all the cultivated land and wasteland were converted to grassland. The land use types were forest land, grassland, water area, residential area, and traffic land.

(3) Scenario 3 (LU-S3): Assuming that all forest land and grassland were converted to cultivated land due to over-farming, the land use types were cultivated land, water area, residential area, transportation land, and wasteland.

(4) Scenario 4 (LU-S4): Assuming that land cover deteriorated seriously. Arable land decreased, and forest land and grassland degraded, while wasteland increased. All the cultivated land, forest land, and grassland were converted into wasteland. The land use types under this scenario were water area, residential area, traffic land, and wasteland.

Table 1. The actual land use types of the river basin and the area distribution of land use types under scenario assumptions (hm^2).

| Land Use Type	Actual Area	Land Use Scenario			
		LU-S1	LU-S2	LU-S3	LU-S4
Cultivated land	19,196	0	0	42,550	0
Woodland	7433	26,746	7433	0	0
Grassland	15,921	15,921	35,234	0	0
Waters	404	404	404	404	404
Residential area	197	197	197	197	197
Residential area (low density)	1094	1094	1094	1094	1094
Traffic land	102	102	102	102	102
Wasteland, bare land	117	0	0	117	42,667

2.4.2. Climate Scenario Assumptions

To a certain extent, runoff was affected by the changes in temperature, precipitation, evaporation, and sunshine hours. Among them, the correlation between runoff and precipitation, temperature, and evaporation was the most obvious. Due to significant positive correlation between evaporation and temperature, we assumed the corresponding climate scenarios by setting different precipitation and temperature conditions and conducted simulations of daily and monthly under different climate scenarios. It was assumed that the temperature was ± 2 °C and ± 1 °C of change, and the precipitation was $\pm 10\%$ and $\pm 25\%$ of change, thus, 24 climate scenarios can be arranged (Table 2). The background temperature was 11 °C and the background precipitation was 540 mm.

Table 2. Assumptions of climate change scenarios.

Temperature	Precipitation				
	−25% (p1)	−10% (p2)	0	+10% (p3)	+25% (p4)
−22% (t1)	C-S1	C-S2	C-S3	C-S4	C-S5
−11% (t2)	C-S6	C-S7	C-S8	C-S9	C-S10
0	C-S11	C-S12	C-S0	C-S13	C-S14
+11% (t3)	C-S15	C-S16	C-S17	C-S18	C-S19
+22% (t4)	C-S20	C-S21	C-S22	C-S23	C-S24

2.5. Technical Route

Firstly, we analyzed the changing characteristics of meteorological elements and hydrological runoff based on meteorological and hydrological data. Then, raster data, meteorological and runoff data were used to construct a regional DEM topographic, land use, soil, and meteorological database. Next, sub-basins and hydrological response units, and established regional SWAT model were divided, and the parameter sensitivity analysis, calibration and simulate were carried out, while the simulation and applicability of the SWAT model in this area were evaluated and discussed. Finally, we simulated the land use and climate change impact on surface runoff using the scenario assumption method. The Figure 4 showed research flowchart.
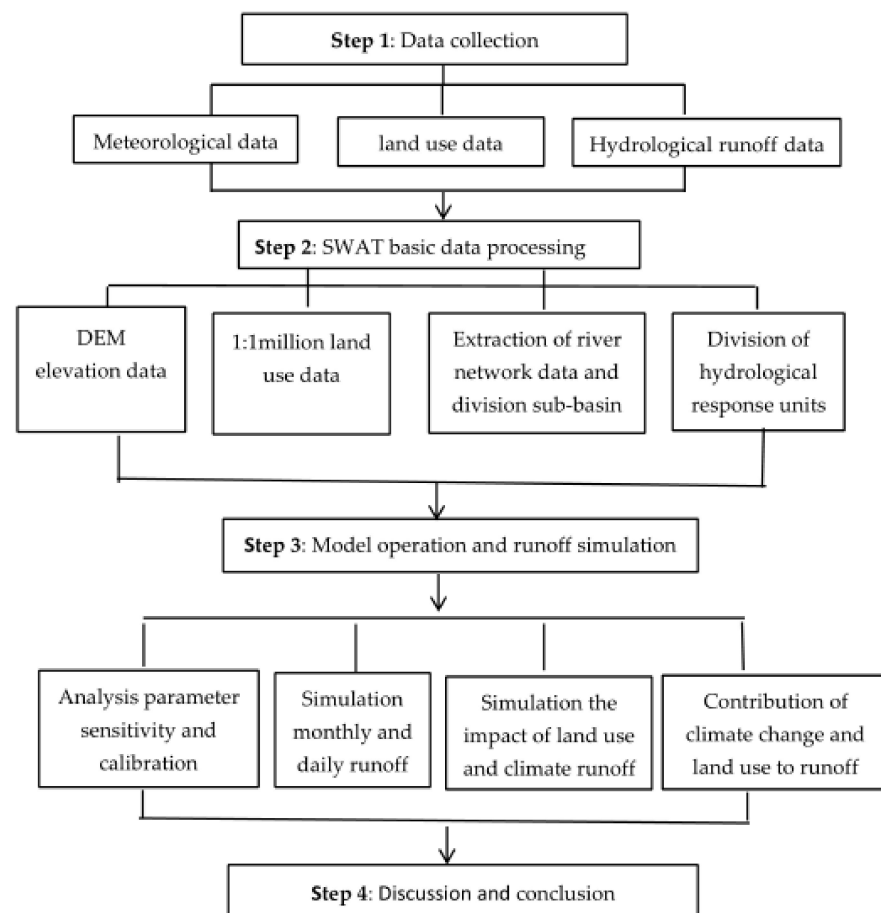
Figure 4. Technical roadmap.

3. Results

3.1. Model Parameter Sensitivity Evaluation

The parameter sensitivity test was an important step to evaluate the results that affect the calibration and verification of the model. In this study, the SUF1-2 algorithm in

SWAT-CUP was used, while the selection of parameters was performed using the Latin hyper-dimension method [19,20], which was calculated by random sampling. Then the selected sensitivity parameters and parameter value ranges were obtained.

In the simulation process of the SWAT model, three time periods of 1976–1978, 1976–1999, and 2001–2019 were set as the model warm-up period, the calibration period, and the verification period, respectively. Through 5 iterations, the 238th of 500 simulations in the last 1 iteration yielded the index was used for evaluation. The sensitivity of parameters in SWAT-CUP was generally selected, while t value and f value were used to evaluate the parameter sensitivity. The f values ranged from 0.00003 to 0.90466 and the t values ranged from 0.12016 to 4.42707. The t value represented the sensitivity, while the f value represented the significance. The smaller the f value, the larger the absolute value of t. Finally, 19 sensitivity parameters were obtained and shown in Table 3. These parameters have been tested with more than 95% reliability. The parameters including base flow regression constant, SCS runoff curve coefficient, and hydraulic conductivity were the most sensitive to effect of the model simulation.

Table 3. Results of parameter sensitivity analysis.

Sort	Parameter Name	Representative Meaning	t Value	f Value
1	CANMX	Maximum canopy interception	4.42707	0.00003
2	CN2	SCS runoff curve coefficient	4.37722	0.00004
3	SOL_K	Saturated hydraulic conductivity	3.19462	0.00200
4	CH_N2	Manning roughness coefficient of main channel	2.40134	0.01865
5	SOL_AWC	Soil available water	2.25788	0.02668
6	SMTMP	Snow melt minimum temperature	1.68142	0.09658
7	CH_K2	Effective hydraulic conductivity of main river bed	1.48910	0.14039
8	GWQMN	Compensation depth of shallow aquifer	1.43892	0.15408
9	GW_DELAY	Groundwater delay time	1.43258	0.15587
10	ALPHA_BNK	Base flow coefficient of river bank regulation and storage capacity	1.25998	0.21134
11	EPCO	Vegetation transpiration compensation coefficient	0.92206	0.35927
12	ALPHA_BF	Base flow regression coefficient	0.86970	0.38707
13	GW_REVAP	Soil reevaporation coefficient	0.79097	0.43130
14	BIOMIX	Biological mixing efficiency factor	0.76520	0.44641
15	SMFMX	Maximum snowmelt coefficient	0.75487	0.45254
16	REVAPMN	Re evaporation coefficient of shallow aquifer	0.72444	0.47091
17	SURLAG	Surface water lag days	0.40663	0.68537
18	TLAPS	Temperature drop rate	0.18854	0.85093
19	ESCO	Soil evaporation compensation factor	0.12016	0.90466

3.2. Flood Simulation Verification

Due to the relatively short duration of the flooding process, it was difficult for the SWAT model to accurately simulate flood events on sub-daily scales. In order to avoid the shortcomings of the existing models, we approximated the daily average flow as the daily maximum peak flow and used the same set of parameters to calibrate the SWAT model. In the simulation, the simulated value of daily average flow was used as the peak flow of floods over the years. Figure 5 showed the daily simulated flow in the upper Weihe River, it can be seen that the variation trend of the simulated value of the flood was consistent with the measured value, while the peaks and valleys of daily runoff were better simulated. Figure 6 revealed the monthly runoff simulation of upper Weihe River; it can be seen that the difference between high and low values of monthly runoff was obvious. The maximum measured runoff in the calibration period on 12 August 1992 was 1570 $m^3 \cdot s^{-1}$, while simulated runoff on that day was 1388.1 $m^3 \cdot s^{-1}$. The measured runoff in flood season was >300 $m^3 \cdot s^{-1}$ higher than that of simulated runoff. The daily simulated runoff in the verification period was also generally less than measured runoff. On 30 August 2000, the measured runoff reached the highest value of 651 $m^3 \cdot s^{-1}$, while the simulated runoff was 591.2 $m^3 \cdot s^{-1}$. When the daily runoff has low values during the calibration period and

verification period, it was found that the simulated runoff of upper Weihe River was higher than the measured average runoff. The average flow difference of the daily simulated runoff and measured runoff in the verification period was 6.19 m^3·s^{-1} and the low value simulation error in both periods was greater than 37%.
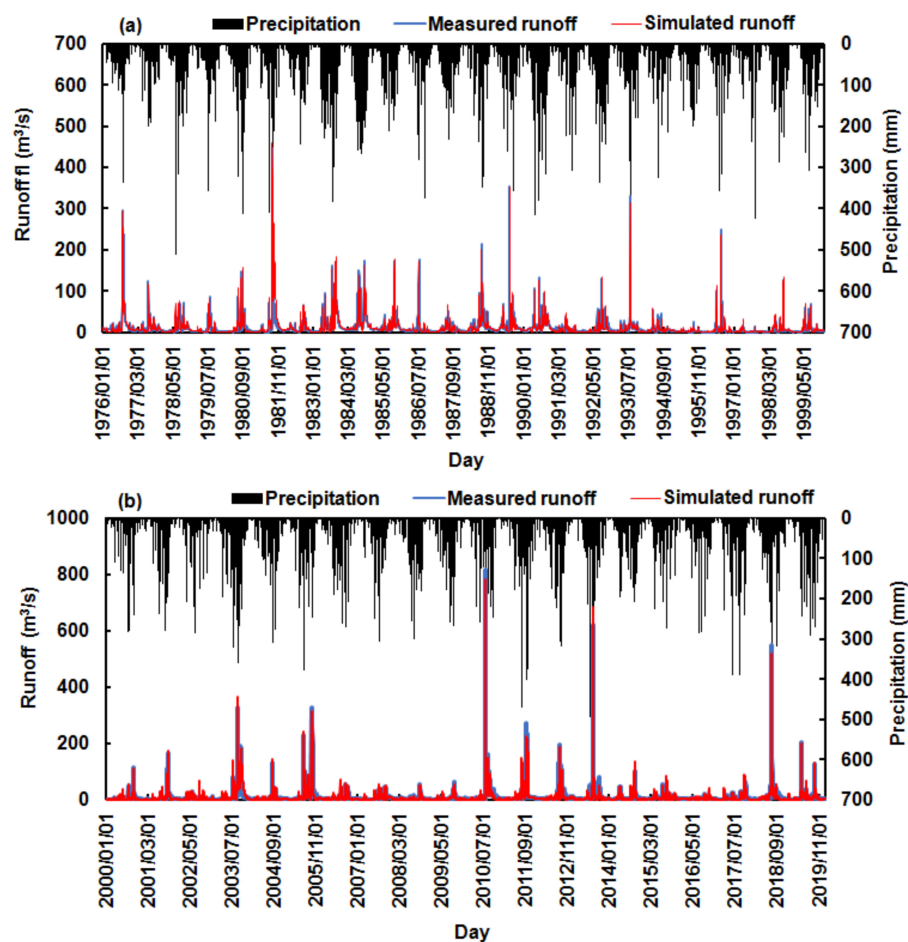
Figure 5. Comparison between daily measured flow and simulated flow in the upper reaches of the Weihe River: (**a**) calibration period and (**b**) verification period.

The inter-annual variation trend of the daily runoff simulation value and the measured value was also consistent. The model can well simulate the runoff from June to October. The largest runoff was in September, the second largest in July. The runoff was smaller in winter. When the runoff had a high value, the average high value of the measured runoff in the calibration period was higher than the average high value of simulation, which was 132.13 m^3·s^{-1} and 124.39 m^3·s^{-1}, respectively. The high value of simulated runoff in the verification period was 79.83 m^3·s^{-1}, which was greater than 76.59 m^3·s^{-1}. The monthly runoff simulation was basically the same as the daily simulation.

Figure 7 illustrates the relationship between the simulated runoff value and the measured value on daily and monthly basis. It shows that the relationship between the two was good, with E$_{NS}$ and R^2 reaching above 0.75 and 0.76, respectively, and PS of less than 13%, achieving high simulation reliability. The relative error of daily runoff simulation was slightly larger than that of monthly simulation. The monthly *p*-factor and *r*-factor values of the calibration period and the validation period were greater than that of daily (Table 4); moreover, *p*-factor and *r*-factor values were in the range of 95upp, and the uncertainty was reduced. As a whole, the monthly simulation effect was better than daily the simulation effect.
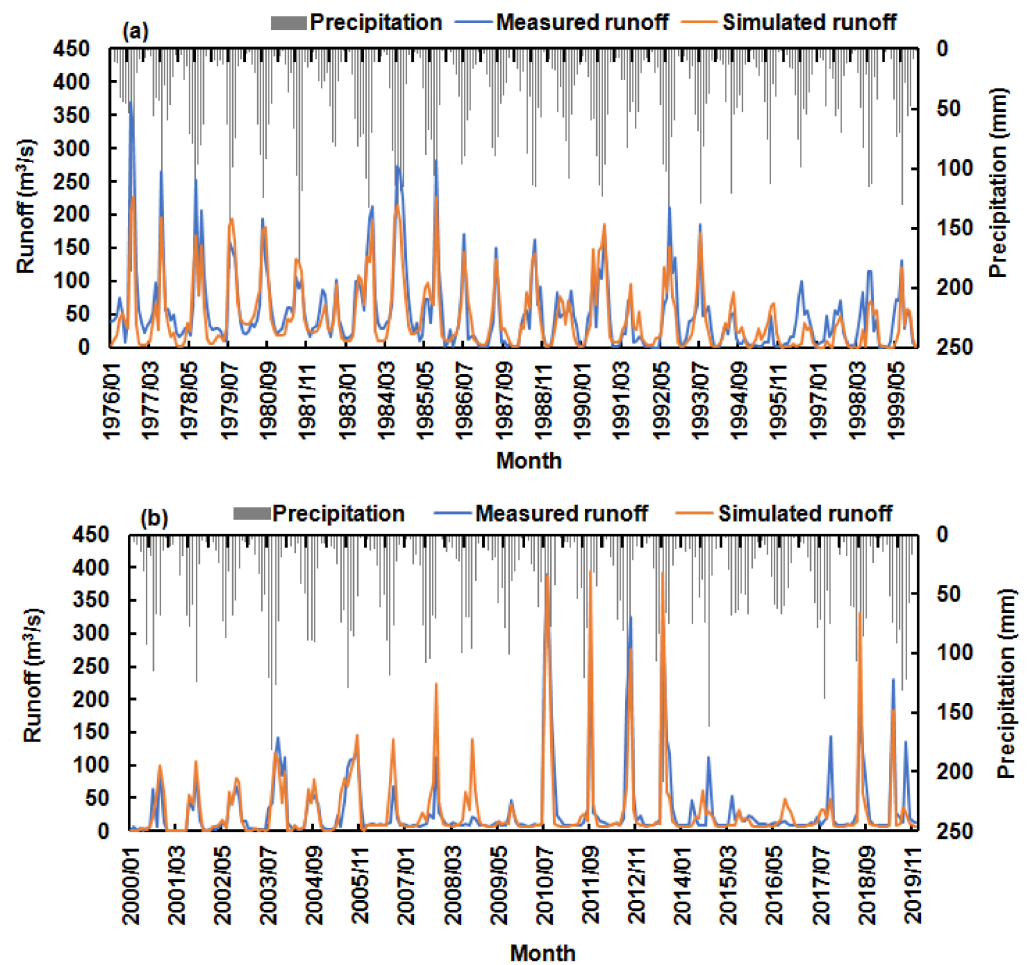
Figure 6. Comparison between monthly measured flow and simulated flow in the upper reaches of the Weihe River: (**a**) calibration period and (**b**) verification period.
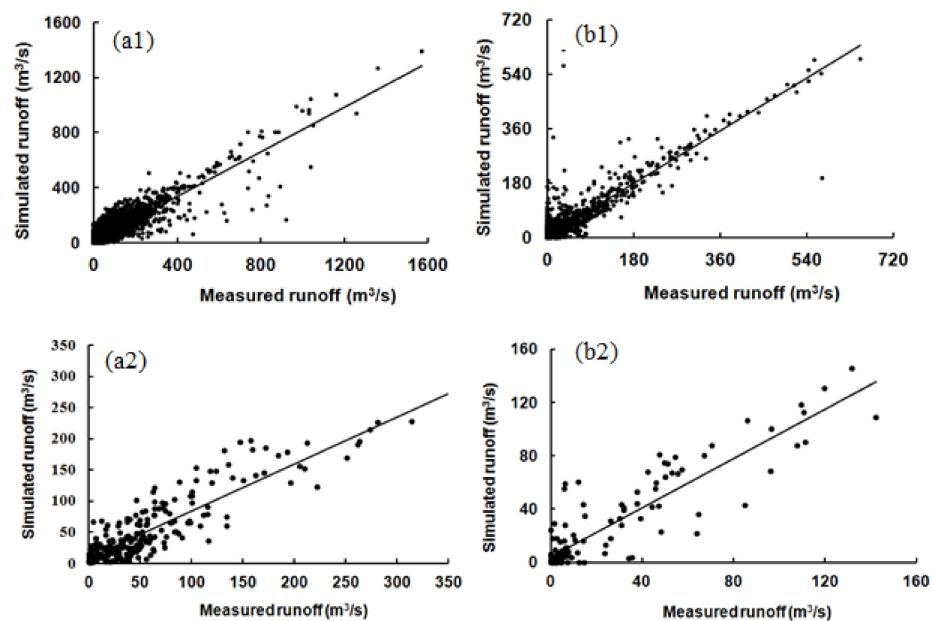

Figure 7. Fitting relationship between the daily simulated runoff and measured runoff: (**a1**) Calibration period and (**b1**) Verification period; the monthly simulated runoff and measured runoff: (**a2**) Calibration period and (**b2**) Verification period.

Table 4. Statistical table of *p*-factor and let-factor analysis results.

Variable	Month		Day	
	p	*r*	*p*	*r*
Calibration period	0.79	0.68	0.74	0.65
verification period	0.77	0.62	0.66	0.68

In order to better simulate the changes of runoff at different levels, according to national river flow test specification (CGB 50179-2015) [37], considering the characteristics of the river, the flood measurement capacity of the station, and various factors that affect the change of the water level and flow, the runoff was divided into 8 levels (see Table 5), Generally, when the flow was greater than 70 m^3·s^{-1}, it was considered that floods may occur in the upper reaches of the Weihe River. It can be seen that the observed daily flood flow probability was basically the same as the simulated daily flood flow probability, and the simulation accuracy rate was over 72%. It can also be seen from the Figure 8, that the daily simulated runoff cumulative probability was basically the same as the observed runoff cumulative probability, and the peak flow of 400 m^3·s^{-1} of daily runoff has been simulated. From 1976 to 2009, floods with more than daily runoff of 200 m^3·s^{-1} were simulated with an accuracy rate of 89%, indicating that the improved SWAT model can simulate the daily flood flow better.
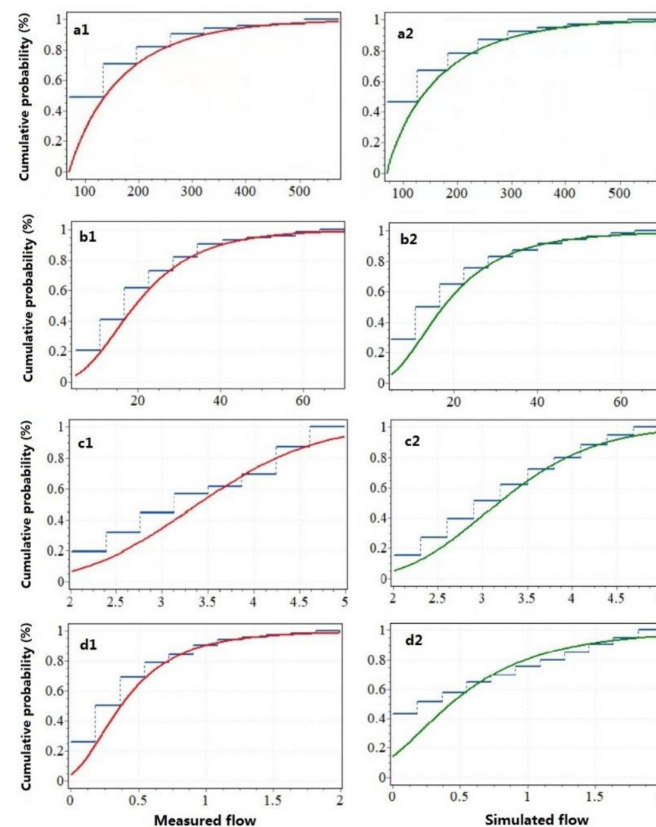
Figure 8. Occurrence probability diagram of measured and simulated daily runoff at different water levels (**a1,a2**) ≥70, 5 ≤ (**b1,b2**) < 70, 2 ≤ (**c1,c2**) < 5, (**d1,d2**) < 2.

Table 5. The number of measured and simulated values of daily runoff at each water level from 1976 to 2019.

| Flow (m^3·s^{-1})	Amount/Times	
Range	Measured Value	Simulated Value
0–2	1833	1613
2–5	876	563
5–70	3144	3538
>70	1452	1591
>100	883	1024
>200	313	314
>300	135	111
>400	76	55

3.3. Simulation of Land Use Impact on Runoff

3.3.1. Impact of Land Use on Runoff

Regional land use reflected the comprehensive utilization of the regional natural environment. The land use changes can change the characteristics of the underlying surface, which has an important impact on the runoff and confluence. Figure 9 shows the distribution of land use types in the study area in 2000, 2005, 2010, and 2015. It can be seen that the proportion of land use types, other than cultivated land showed a generally rising trend. Among them, grassland and urban and rural land showed a more significant increase. From 2000 to 2015, the total proportion of grassland in all land types increased from 35.36% to 35.81%, while the proportion of residential land increased from 2.47% to 2.9%. During this period, the policy of returning arable land to forests significantly reduced the arable land, but the total proportion of the farmland was still the highest, while the area of woodland, grassland, and waters increased significantly. Meanwhile, with the social development and technological improvement, the residential areas (including low-density residential areas) and traffic land increased at a very rapid rate. Their proportions of residential areas and traffic land increased from 2.6% and 0.08% to 2.9% and 0.23%, respectively.
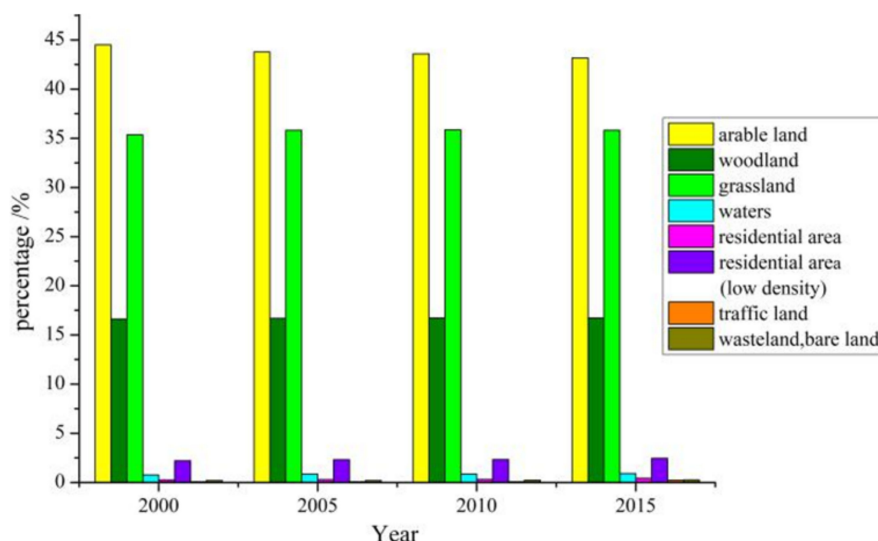
Figure 9. Proportions of land use types in different years.

By simulating the runoff in the land use context in different periods, it was found that the total amount and change trend of the simulated runoff in the land use context in the periods of 2000, 2005, 2010, and 2015 existed some differences (Figure 10), while the average simulated runoff of upper Weihe River decreased from 2000 to 2015 in the land use context.
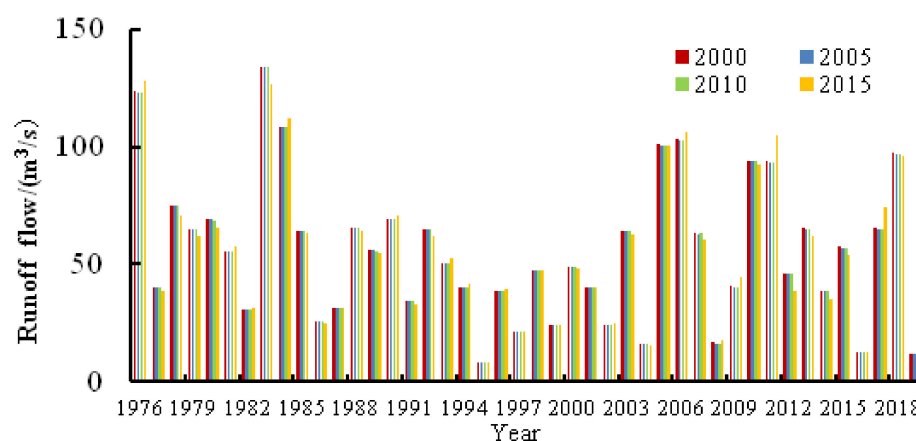
Figure 10. Change trends of simulated runoff changes in the land use context in different years.

3.3.2. Runoff Simulation under Land Use Scenario Assumptions

To further understand the impact of human activities on floods, we used four established extreme land use scenarios to simulate the contribution of land type conversion to runoff. Taking 2015 as the benchmark, under the LU-S1, LU-S2, LU-S3, and LU-S4 land type conversion scenarios, the annual runoff simulation was shown in Figure 11. It can be seen that the annual average simulated runoff of upper Weihe River under LU-S1, LU-S2, and LU-S3 scenarios were 47.83 $m^3 \cdot s^{-1}$, 52.18 $m^3 \cdot s^{-1}$, and 57.95 $m^3 \cdot s^{-1}$, respectively, with the largest value of 101.45 m^3/s under the LU-S4 scenario. Compared with the average runoff under the background of land use in 2015, the simulated runoff decreased by 11.52% and 3.48% under LU-S1 and LU-S2 scenarios, respectively, and increased by 7.2% and 87.66% under LU-S3 and LU-S4 scenarios, respectively. It was believed that the change of forest land and grassland had relatively little effect on regional runoff, and the rate of runoff change was less than 12%. The increase of forest land and grassland would reduce the regional surface runoff, the expansion of cultivated land would increase the runoff, while the expansion of wasteland could significantly increase the surface runoff. Figure 12 displayed the monthly runoff simulation of the four land use scenarios, it can be seen that the maximum average runoff at LU-S4 was 109.78 m^3/s. In this scenario, the flood season runoff was significantly larger than another three scenarios. However, the simulated runoff values under the LU-S1, LU-S2, and LU-S3 scenarios were relatively small. Among them, the simulated monthly runoff of LU-S3 was relatively large, which was 62.22 $m^3 \cdot s^{-1}$. Similarly, compared with the average runoff under the background of land use in 2015, under the LU-S1 and LU-S2 scenarios, the runoff change rates were −7.06% and −4.8%, respectively. Under LU-S3 scenario, the increase of cultivated land led to the increase of the monthly runoff by 7.89%, and the increased range of runoff under the LU-S4 scenario was more than 90%. It can be seen that the increase of forest land and grassland also weakened the runoff to a lesser extent in the simulation of monthly runoff. The expansion of cultivated land increased the surface runoff, while the wasteland still had a significant influence. The gap between the abundance and dryness of the runoff was aggravated, while the seasonal change was more obvious.
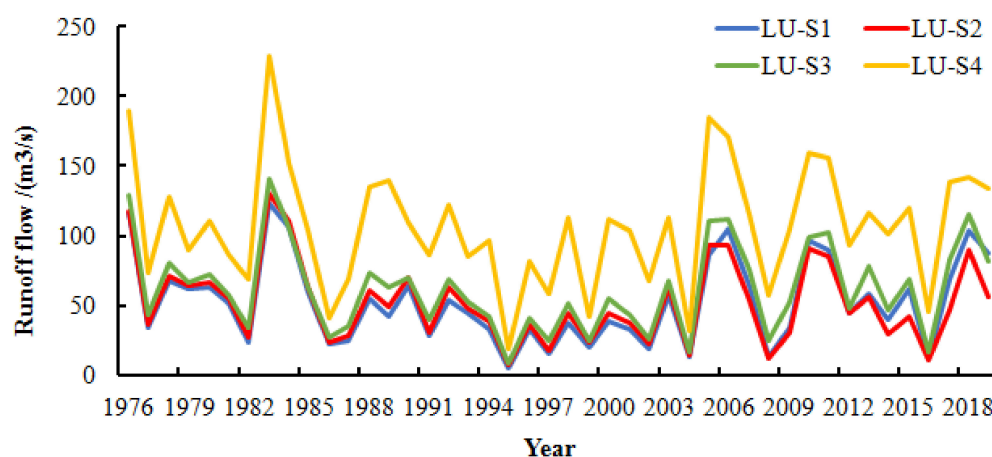
Figure 11. Comparison of simulated annual runoff trends under different land use scenarios.
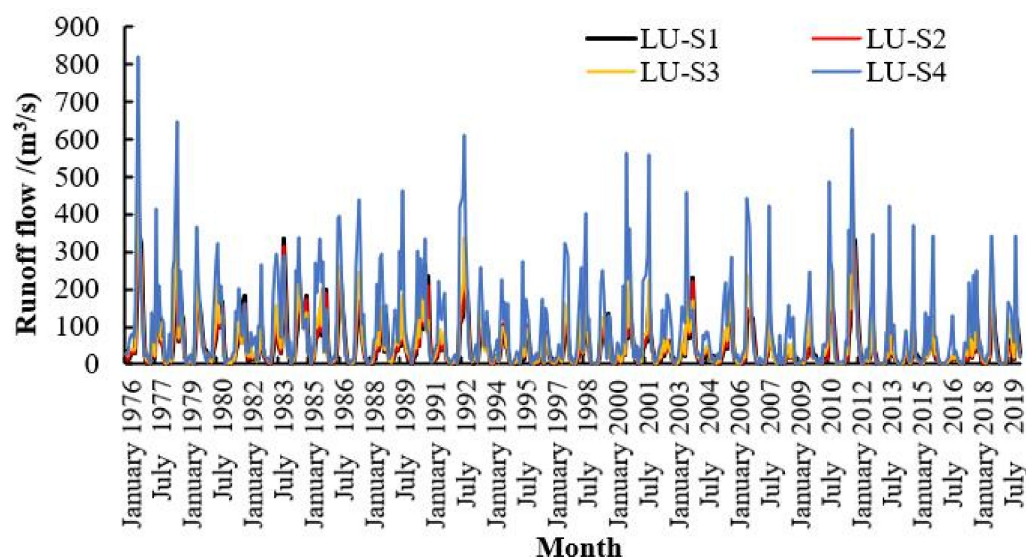

Figure 12. Comparison of simulated monthly runoff trends under different land use scenarios.

3.4. Simulation of Climate Change Impact on Runoff

3.4.1. Runoff Simulation under Climate Scenario

In order to further explore the degree of response of runoff to climate change, the precipitation and temperature data under 24 climate scenarios were input into the SWAT model to obtain the annual average simulated runoff under each climate scenario, as shown in Table 6 and Figure 13. It can be seen that the increase in precipitation increased the runoff, while the increase in temperature weakened the runoff. Even if the temperature changes, the runoff was always the largest under the scenario of a 25% increase in precipitation. However, when the precipitation conditions remain unchanged, the runoff was larger at low temperature. In all hypothetical scenarios, when the temperature decreased by 22% and the precipitation increased by 25%, the runoff was the largest. At this time, the annual average simulated runoff reached 133.63 m^3·s^{-1}. In contrast, the smallest runoff was obtained under the scenario of a 22% increase in temperature and a 25% decrease in precipitation, while the annual average simulated runoff was 14.93 m^3·s^{-1}. When the temperature conditions remained unchanged and the precipitation decreased by 10%, the simulated runoff was reduced by 16.4 m^3·s^{-1}, on average. When the precipitation increased by 10%, the runoff increased by 22.53 m^3·s^{-1}. When the precipitation condition remained constant, the temperature increased by 11%, while the annual runoff decreased by 5.45 m^3·s^{-1}, on average. When the temperature decreased by 11%, the average increase of

runoff was 6.16 m³·s⁻¹. When the temperature remained unchanged and the precipitation decreased by 10%, the annual runoff decreased by 17.7 m³·s⁻¹. When the precipitation increased by 10%, the runoff increased by 21.6 m³·s⁻¹. When the precipitation remained unchanged and the temperature increased by 11%, the runoff decreased by 5.9 m³·s⁻¹. When the temperature decreased by 11%, the runoff increased by 6.71 m³·s⁻¹. Overall, the change of precipitation led to a greater change rate of the annual runoff, while the temperature change had a smaller impact on the change rate. In addition, under climate conditions, the runoff was more obviously affected by the increase of precipitation.

Table 6. Annual average simulated runoff of under different climate scenarios (m³·s⁻¹).

Temperature	Precipitation				
	P1	**P2**	**0**	**P3**	**P4**
t1	23.43	46.73	68.76	92.41	133.63
t2	20.32	40.84	60.82	82.87	122.53
0	18.58	36.41	54.11	75.71	114.01
t3	16.29	31.65	48.21	67.94	105.03
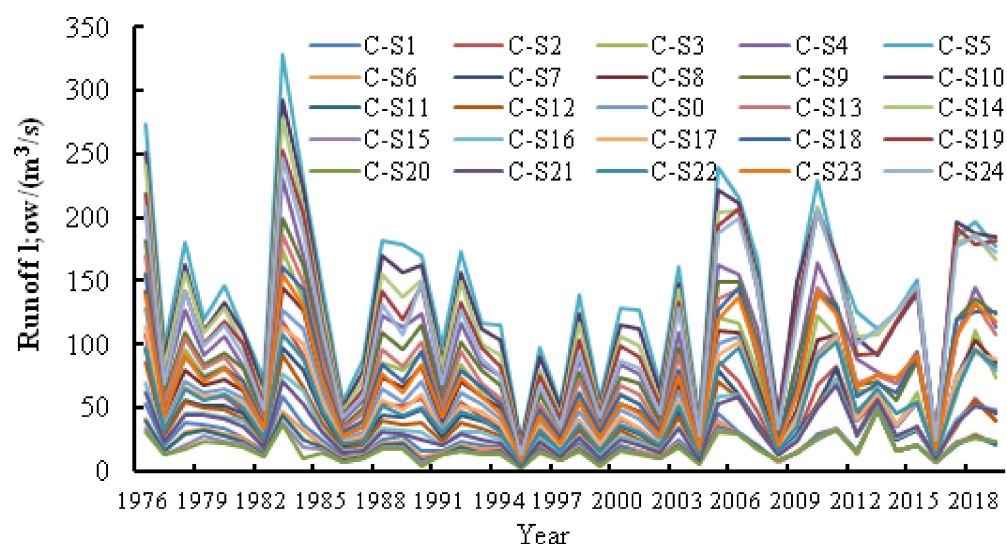
Figure 13. Variation trend of annual simulated runoff under different climate scenarios.

Table 7 showed the simulation results of monthly runoff under the climate scenario. It can be seen that the surface runoff of upper Weihe River reached the maximum value of 144.53 m³·s⁻¹ in climate scenario of CS-5, and the minimum value of 16.91 m³·s⁻¹ in climate scenario of C-20. When the temperature remained unchanged and the precipitation decreased or increased by 10%, the average change of monthly runoff was −17.17 m³·s⁻¹ or 24.16 m³·s⁻¹, respectively. When the precipitation remained unchanged and the temperature increased by 11%, the average decrease of runoff of upper Weihe River was 5.71 m³·s⁻¹. When the temperature decreased by 11%, the average increase of monthly runoff was 7.21 m³·s⁻¹. When the temperature remained unchanged and the precipitation decreased by 10%, the monthly runoff of upper Weihe River decreased by 18.97 m³·s⁻¹. In contrast, when the precipitation increased by 10%, the monthly runoff increased by 21.6 m³·s⁻¹. When the precipitation remained unchanged and the temperature increased or decreased by 11%, the runoff of upper Weihe River decreased by 6.4 m³·s⁻¹ or increased by 7.41 m³·s⁻¹, respectively. Overall, in the monthly runoff simulation under 24 climate scenarios, the change in precipitation was still an important factor of changing the runoff, and the increase in runoff was greater than the decrease of runoff.

Table 7. The monthly average simulated runoff at Linjiacun Station under different climate scenarios ($m^3 \cdot s^{-1}$).

Temperature	Precipitation				
	p1	**p2**	**0**	**p3**	**p4**
t1	25.62	50.14	73.26	98.82	144.53
t2	22.6	44.04	65.08	89.02	132.71
0	20.28	38.7	57.67	79.93	121.78
t3	18.42	33.99	51.27	72.24	112.83
t4	16.91	30.45	45.94	65.57	104.51

3.4.2. Runoff Simulation Prediction under Climate Influence

In recent years, with the continuous increase of greenhouse gas CO_2 emissions, the global temperature continues to rise, which has a greater impact on the runoff. In order to understand the runoff of the Weihe River Basin in the next 100 years, two climate scenarios of RCP2.6 and RCP8.5 were used to simulate the runoff change of the upper Weihe River in the next 100 years. The simulation results were shown in Figure 14. It showed that the simulated runoff under the low-emission of RCP2.6 scenario is greater than that under the high-emission scenario of RCP8.5, indicating that the flow could be reduced under the high-emission scenario. The runoff trend slightly decreases over time. According to the forecast, the maximum runoff may occur in 2050, 2080, and 2090, while the possibility of flood disasters is relatively high. In 2030, 2070, and 2100, the runoff will decrease significantly. In the high emission of RCP8.5 the runoff is more pronounced than the low-emission RCP2.6 runoff reduction.
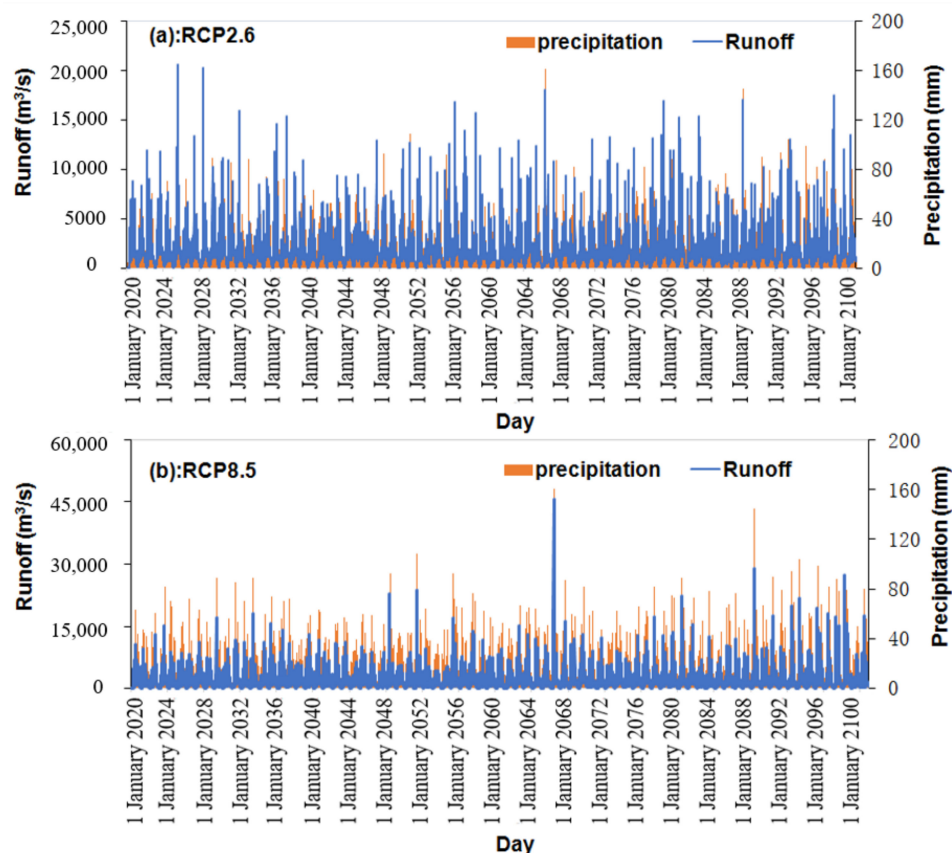
Figure 14. Runoff and precipitation prediction under the greenhouse gas emission scenarios of RCP2.6 (**a**) and RCP8.5 (**b**).

3.5. Contribution Rate of Climate Change and Land Use Type to Runoff

In order to further discuss the impact of land use types and climate change on runoff changes in various periods, the contribution of land use and climate change to runoff was examined. The cumulative slope change rate comparison method was used to calculate the impact of precipitation and human activities on runoff [38,39]. According to Equations (6)–(8), the calculation of contribution of land use and climate change to runoff were obtained, as shown in Table 8. It shows that since the 1970s, the land use types have become the main factor to affect the reduction of runoff in the upper reaches of the Weihe River, i.e., the runoff was less influenced by land use type before the 1970s, but it was more affected by climate change and human activities in the latter two periods. Since the 1970s, the impact of land use types on runoff has been increasing. After the 1990s, the temperature in the upper Weihe River experienced a sudden increase, while the precipitation continued to decrease, which had a greater impact on runoff. From 1971 to 1993, the contribution rate of climate change to runoff reduced by 6.21%, and the contribution rate of human activities to runoff reduced by 93.79%. Thus, it can be concluded that the runoff changes of the main stream of the Weihe River were greatly affected by human activity changes, and both changes were above 90%. From 1994 to 2015, land use types were still the main factor to affect the runoff reduction, and the contribution rate was 74.72%, which was smaller than the contribution rate from 1971 to 1993. Before 1993, the contribution rate of natural climate to the runoff reduced to less than 10% and then increased to more than 25%. This maybe because many large-scale water conservancy and soil conservation projects have been built in the upper Weihe River since the 1970s. Man-made storage has become the main factor for the reduction of runoff. The sudden rise of temperature since the 1990s has increased the potential evapotranspiration and its contribution to the reduction of runoff. As a result, the contribution rate of climate change to the reduction of runoff has increased. At the same time, the scale of large-scale water conservancy and soil conservation projects in the middle reaches of the Weihe River has saturated in recent years, causing the impact of human activities on runoff to stabilize and the impact to significantly decline.

Table 8. The contribution rate of climate change and human activities to runoff changes.

Periods	Runoff/mm	Precipitation/mm	Potential Evaporation/mm	C_E/%	C_P/%	$(C_E + C_P)$/%	C_H/%
1960–1970	31.42	655	1348	–	–	–	–
1971–1993	16.11	625.5	1314	−5.39	11.6	6.21	93.79
1994–2015	5.93	585.9	1467	12.98	12.3	25.28	74.72

4. Discussion

The SWAT model was used to simulate the runoff in the upper Weihe River, while land use and climate scenario assumptions were proposed to analyze the impact of land use and climate changes on the runoff. The simulations showed that parameters, such as the CANMX, CN2, SOL_K, CH_N2, and SOL_AWC, were the most sensitive among the 19 sensitivity parameters established. When the runoff was high, the simulation error was small, and when the daily runoff was low, the simulation error was large, which were basically consistent with existing studies [38,39]. However, the error of this study was smaller than that of existing studies. Compared with the existing studies [40–42], the reason may be the fact that, during the simulation process, all sub-watersheds were carefully designed and the soil types were carefully divided, which led to a certain difference in the simulation effect of upstream to a certain extent. Due to the influence of the surface environment on the runoff simulation, the simulation uncertainty was caused by various error sources.

For simulating the peak flow of floods in the upper Weihe River to avoid the shortcomings of the existing models, we used the improved SWAT model with an hourly step size to simulate more than the peak flow of 400 $m^3 \cdot s^{-1}$ of daily runoff in the upper reaches of the

Weihe River. The simulation accuracy meets the requirements of the Hydrological Information Forecasting Specification (GB/T22482-2008) well, which showed that the improved SWAT can be used for flood simulation research in the basin. Furthermore, the results were basically consistent with the flood simulation results by Qin et al. [43]. Compared with the distributed VIC, DHSVM model [43,44] and the traditional SWAT model [36], it has better advantages, and the model application was simple, and can be used to directly revise the designed flood to reduce uncertainty in simulation parameters, thereby improving the accuracy of simulation effect during the validation period.

Adopting the sequential uncertainty fitting algorithm (SUFI-2) in the model simulation parameter calibration process, compared with the generalized likelihood uncertainty estimation (GLUE) method [45], and the parameter solving (ParaSol) method [46], the accuracy of the model simulation was improved, and the uncertainty of the simulation was reduced. Moreover, the model can well simulate the variation of water production in the Weihe River and has good applicability to simulating runoff and analyzing the influencing factors under hypothetical land use and climate scenarios. Based on land use scenarios, simulation showed that the increase of forest and grassland will reduce surface runoff to a certain extent, while the expansion wasteland will increase surface runoff, while the impact of wasteland was the most obvious. It was found that the increase in the area of woodland and grassland weakened the runoff, but the impact was relatively small. These results were basically consistent with those of Li et al. [47] and Ge et al. [48]. Although the land cover types under the LU-S1 and LU-S2 scenarios had changed, there were still woodlands and grasslands. Surface vegetation can absorb, intercept, and evaporate runoff. However, under the LU-S4 scenario, there was no vegetation on the surface. The interception effect of runoff was greatly reduced, and the surface water increased so that the total surface runoff under this scenario was also higher than the other three scenarios. Therefore, the effects of vegetation coverage on runoff interception and transpiration were important influencing factors for surface runoff and flood.

Decomposing the contribution of human activities and climate change to runoff showed that the contribution rate of human activities to the runoff change in the upper Weihe River was relatively large. The area of arable land continued to decrease, while the forest land, bare land, traffic land, water area, and construction land continued to increase. The grassland area increased first and then decreased from 2000 to 2015 in the upper Weihe River. It can be seen that the increase of forest land and grassland area can weaken the runoff combined with the analysis of simulated runoff under different scenarios, but the impact was relatively small. The increase of cultivated land and wasteland area can accelerate the surface runoff. This result is consistent with that of Mewded et al. [49]. It can be concluded that the uneven temporal and spatial distribution of precipitation, as well as specific topographic conditions and water system characteristics are the inducing mechanisms of frequent flood disasters in the upper Weihe River. Heavy rain and the resulting disaster chain aggravated the intensity of flood disasters in the upper Weihe River, while the disturbance of human activities and weak disaster resistance amplify the flood disasters. Therefore, these are the most effective ways to prevent floods by reducing the area of arable and wasteland, increasing the area of grassland and woodland, and improving the resilience of the region.

Overall, in order to improve the accuracy of the simulation, in the process of model calibration, combining of measured runoff, probability statistics, and improved SWAT model parameters, this study simulated the potential impact of climate change and land use type changes on runoff in the watershed, thus revealing the impact of land use and climate change on the risk of floods in the future. Of course, the change of hydrological runoff is affected by many factors, such as geographical location, topography, vegetation soil, topography and hydrogeological conditions, and climate change. More detailed and in-depth studies are needed on flood simulation and influencing factors so as to provide a certain reference for water resources management in the basin.

5. Conclusions

In this paper, the SWAT model was used to simulate the runoff in the upper Weihe River. The scenario method was used to analyze the response of runoff to land use and climate changes, while the cumulative slope change rate comparison method was employed to calculate the impact of precipitation and human activities on runoff. The conclusions were as follows:

The simulation results of monthly and daily runoff upper Weihe River verified the applicability of the SWAT model in this study area. The improved SWAT model has good applicability in flood simulation in the upper Weihe River. The accuracy rate of the simulated daily runoff of 400 $m^3 \cdot s^{-1}$ reaches 72%, demonstrating that the SWAT model can be used to simulate the timing and pattern of flood occurrence in the upper Weihe River. The change of land use type has a certain impact on surface runoff, while the change of surface runoff was mainly affected by the absorption, interception, and transpiration of vegetation, and can be used for flood simulation research in this watershed.

The change of climate conditions also has a certain impact on surface runoff. The contribution rate of human activities to runoff reduction was greater than that of climate change, but the contribution rate of climate change has increased in recent years. Reducing the impact of human activities on runoff is an important way to achieve the hydrological cycle.

The simulation result of the impact of land use change on runoff showed that the increase of forest land and grassland reduced surface runoff to a certain extent, while the expansion of cultivated land and wasteland increased surface runoff. The precipitation changes have a greater impact on runoff than temperature, while the increase in runoff caused by climate change was greater than the decrease of runoff. Simulation results provided basis for comparison of different regions. Of course, the SWAT model can be applied only when the parameters were modified in other watersheds.

References

1. Yazdani, M.; Mojtahedi, M.; Loosemore, M.; Sanderson, D. A modelling framework to design an evacuation support system for healthcare infrastructures in response to major flood events. *Prog. Disaster Sci.* **2022**, *13*, 100218. [CrossRef]
2. Ishiwatari, M.; Sasaki, D. Investing in flood protection in Asia: An empirical study focusing on the relationship between investment and damage. *Prog. Disaster Sci.* **2021**, *12*, 100197. [CrossRef]
3. Shreevastav, B.B.; Tiwari, K.R.; Mandal, R.A.; Nepal, A. Assessing flood vulnerability on livelihood of the local community: A case from southern Bagmati corridor of Nepal. *Prog. Disaster Sci.* **2021**, *12*, 100199. [CrossRef]
4. Xia, J.; Qiu, B.; Pan, X.Y.; Weng, J.W.; Fu, G.B.; Ouyang, R.L. Water resources vulnerability assessment method and its application under the influence of climate change. *Adv. Ear. Sci.* **2012**, *27*, 443–451.
5. Lei, X.H.; Wang, H.; Liao, W.H.; Yang, M.X.; Gui, Z.L. Research progress of meteorological and hydrological forecasting under changing environment. *J. Hydrol. Eng.* **2018**, *49*, 9–18.
6. Liu, Y.G.; Wang, N.L.; Zhang, J.H.; Wang, L.G. Climate change and its impacts on mountain glaciers during 1960–2017 in western China. *J. Arid Land.* **2019**, *11*, 537–550. [CrossRef]
7. Tudose, N.C.; Cremades, R.; Broekman, A.; Sanchez-Plaza, A.; Marin, M. Mainstreaming the nexus approach in climate services will enable coherent local and regional climate policies. *Adv. Clim. Chang. Res.* **2021**, *12*, 752–755. [CrossRef]
8. Marin, M.; Clinciu, I.; Tudose, N.C.; Ungurean, C.; Cacovean, H. Assessing the vulnerability of water resources in the context of climate changes in a small forested watershed using swat: A review. *Environ. Res.* **2020**, *184*, 109330. [CrossRef]
9. Jiang, X.; Liang, Z.; Qian, M.; Zhang, X. Method for probabilistic flood forecasting considering rainfall and model parameter uncertainties. *J. Hydrol. Eng.* **2019**, *24*, 04019056. [CrossRef]
10. Praskievicz, S.; Chang, H. A review of hydrological modelling of basin-scale climate change and urban development impacts. *Prog. Phys. Geogr.* **2009**, *33*, 650–671. [CrossRef]

11. Dwarakish, G.S.; Ganasri, B.P.; De Stefano, L. Impact of land use change on hydrological systems: A review of current modeling approaches. *Cogen. Geosci.* **2015**, *1*, 1115691. [CrossRef]

12. Pongpetch, N.; Suwanwaree, P.; Yossapol, C.; Dasananda, S.; Kongjun, T. Using SWAT to Assess the Critical Areas and Nonpoint Source Pollution Reduction Best Management Practices in Lam Takong River Basin, Thailand. *Environ. Asia* **2015**, *8*, 41–52.

13. Jung, C.G.; Kim, S.J. Assessment of the water cycle impact by the Budyko curve on watershed hydrology using SWAT and CO_2 concentrations derived from Terra MODIS GPP. *Ecol. Eng.* **2018**, *118*, 179–190. [CrossRef]

14. Golmohammadi, G.; Rudra, R.; Dickinson, T.; Goel, P.; Veliz, M. Predicting the temporal variation of flow contributing areas using SWAT. *J. Hydrol.* **2017**, *547*, 375–386. [CrossRef]

15. Lucas-Borja, M.E.; Carrà, B.G.; Nunes, J.P.; Bernard-Jannin, L.; Zimbone, S.M. Impacts of land-use and climate changes on surface runoff in a tropical forest watershed (Brazil). *Hydrol. Sci. J.* **2020**, *65*, 1956–1973. [CrossRef]

16. Amin, A.; Nuru, N. Evaluation of the Performance of SWAT Model to Simulate Stream Flow of Mojo River Watershed: In the Upper Awash River Basin, in Ethiopia. *Hydrology* **2020**, *8*, 7. [CrossRef]

17. Shrestha, S.; Sattar, H.; Khattak, M.S.; Wang, G.; Babur, M. Evaluation of adaptation options for reducing soil erosion due to climate change in the Swat River Basin of Pakistan. *Ecol. Eng.* **2020**, *158*, 106017. [CrossRef]

18. Gao, X.; Yan, C.; Wang, Y.; Zhao, X.; Zhao, Y.; Sun, M.; Peng, S. Attribution analysis of climatic and multiple anthropogenic causes of runoff change in the Loess Plateau—A case-study of the Jing River Basin. *Land Degrad. Dev.* **2020**, *31*, 1622–1640. [CrossRef]

19. Chen, N.; Chen, N.; Zhang, N.; Hou, N.; Shen, N.; Chen, N. Impacts of climate change and LULC change on runoff in the Jinsha River Basin. *J. Geogr. Sci.* **2020**, *30*, 85–102. [CrossRef]

20. Yuan, Y.Z.; Zhang, Z.D.; Meng, J.H. Impact of changes in land use and climate on the runoff in Liuxihe Watershed based on SWAT model. *Chin. J. Appl. Ecol.* **2015**, *26*, 989–998.

21. Liu, Y.G.; Yu, K.K.; Zhao, Y.Q.; Bao, J.C. Impacts of Climatic Variation and Human Activity on Basin Runoff in Western China. *Sustainability* **2022**, *14*, 942. [CrossRef]

22. Jiang, C.; Xiong, L.; Wang, D.; Liu, P.; Guo, S.L.; Xu, C.Y. Separating the impacts of climate change and human activities on runoff using the Budyko-type equations with time-varying parameters. *J. Hydrol.* **2015**, *522*, 326–338. [CrossRef]

23. Goswami, P.; Sharma, A. Climate Change Effects on Water Availability. *Asian J. Environ. Sci.* **2015**, *10*, 57–61. [CrossRef]

24. Ning, Y.N.; Yang, X.N.; Sun, W.Y. The trend of runoff change and its attribution in the middle reaches of the Yellow River. *J. Nat. Res.* **2021**, *36*, 256–269. [CrossRef]

25. Jha, M.; Pan, Z.; Takle, E.S.; Gu, R. Impacts of climate change on streamflow in the upper Mississippi River Basin: A regional climate model perspective. *J. Geophys. Res. Atmos.* **2004**, *109*, D09105. [CrossRef]

26. Li, L.; Ni, J.R.; Chang, F.; Yue, Y.; Frolova, N.; Magritsky, D.; Borthwick, A.G.L.; Ciais, P.; Wang, Y.; Zheng, C.; et al. Global trends in water and sediment fluxes of the world's large rivers. *Sci. Bull.* **2020**, *65*, 62–69. [CrossRef]

27. Fan, C.H. The formation mechanism of China's water resources public policy: Experience, problems and countermeasures. *China Popul. Resour. Environ.* **2015**, *25*, 94–98.

28. Feng, W.; Bai, Y.; Zhang, Y.; Li, Z. Balancing water demand for the Heihe River Basin in Northwest China. *Phys. Chem. Earth Parts A/B/C* **2017**, *101*, 178–184.

29. Amit, R.J. China's water problems. *Asian Aff.* **2018**, *49*, 645–658.

30. Bian, J.M.; Wang, S.J.; Lin, N.F.; Tang, J. Research on the evolution of runoff and its influence mechanism in the Huolin River Basin in semi-arid areas. *Resour. Environ. Arid. Areas* **2004**, *18*, 4.

31. Hagen, J.S.; Cutler, A.; Trambauer, P.; Weerts, A.; Suarez, P.; Solomatine, D. Development and evaluation of flood forecasting models for forecast-based financing using a novel model suitability matrix. *Prog. Disaster Sci.* **2020**, *6*, 100076. [CrossRef]

32. Konapala, G.; Mishra, A.K. Three-parameter based streamflow elasticity model: Application to MOPEX basins the USA at annual and seasonal scales. *Hydrol. Earth Syst. Sci. Discuss.* **2016**, *20*, 2545–2556. [CrossRef]

33. Srivastava, K.K.; Abbi, S.D.S.; Loe, B.R. Estimation of water balance of lower Sutlej catchment up to Bhakra dam site by Thornthwaite's method. *MAUSAM* **1977**, *28*, 507–514. [CrossRef]

34. Abbaspour, K.C.; Johnson, C.A.; van Genuchten, M.T. Estimating Uncertain Flow and Transport Parameters Using a Sequential Uncertainty Fitting Procedure. *Vadose Zone J.* **2004**, *3*, 1340–1352. [CrossRef]

35. Abbaspour, K.C.; Rouholahnejad, E.; Vaghefi, S.; Srinivasan, R.; Yang, H.; Kløve, B.A. Continental-scale hydrology and water quality model for Europe: Calibration and uncertainty of a high-resolution large-scale SWAT model. *J. Hydrol.* **2015**, *524*, 733–752. [CrossRef]

36. Thavhana, M.P.; Savage, M.J.; Moeletsi, M.E. SWAT model uncertainty analysis, calibration and validation for runoff simulation in the Luvuvhu River catchment, South Africa. *Phys. Chem. Earth* **2018**, *105*, 115–124. [CrossRef]

37. Wan, R.R.; Yang, G.S. Discussion on some issues in the study of hydrological effects of LUCC in watershed. *Prog. Geogr. Sci.* **2005**, *3*, 25–33.

38. Xiong, B.F. Analysis of water level (flow) classification of Wuguan hydrological station. *Shaanxi Water Res.* **2019**, *5*, 52–53, 55.

39. Ren, L.; Xue, L.Q.; Liu, Y.H. Study on variations in climatic variables and their influence on runoff in the Manas River Basin, China. *Water* **2017**, *9*, 258. [CrossRef]

40. Wang, J.S.; Yan, Y.X.; Yan, M.; Zhao, X.K. Contributions of Precipitation and Human Activities to the Runoff Change of the Huangfuchuan Drainage Basin:Application of Comparative Method of the Slope Changing Ratio of Cumulative Quantity. *Acta Geogr. Sin.* **2012**, *67*, 388–397.

41. Bormann, H. Regional hydrological modelling in Benin (West Africa): Uncertainty issues versus scenarios of expected future environmental change. *Phys. Chem. Earth.* **2005**, *30*, 472–484. [CrossRef]

42. Arabi, M.; Govindaraju, R.S.; Hantush, M.M. A probabilistic approach for analysis of uncertainty in the evaluation of watershed management practices. *J. Hydrol.* **2007**, *333*, 459–471. [CrossRef]

43. Qin, Z.X.; Peng, T.; Wang, J.B.; Dong, X.H.; Chang, W.J.; Ma, H.B.; Liu, J.; Wang, G.X. Revision of design flood in the upper Huaihe basin based on SWAT model. *Lake Sci.* **2021**, *33*, 595–606.

44. Yang, J.; Reichert, P.; Abbaspour, K.C.; Xia, J.; Yang, H. Comparing uncertainty analysis techniques for a SWAT application to the Chaohe Basin in China. *J. Hydrol.* **2008**, *358*, 1–23. [CrossRef]

45. Wen, Y.H.; Li, Z.J.; Huo, W.B.; Zhang, H.C.; Tong, B.X. Research on parameter uncertainty of GLUE method based on different objective functions. *Hydropower* **2018**, *44*, 10–16.

46. Chen, H.T.; Cao, X.Z. Comparative analysis of the results of parameter optimization methods based on the most suitable confidence interval of SUFI-2 parameters. *Water-Sav. Irrig.* **2021**, *6*, 24–30.

47. Li, Z.J.; Liu, J.Y.; Lu, C.X.; Suning. Analysis of the relationship between landscape pattern and runoff in the Yihe River Basin based on land use change. *J. China Agric. Univ.* **2020**, *25*, 9.

48. Ge, Z.N.; Hao, J.; Ju, Q. The impact of land use change on runoff in the Weihe River Basin. *People Yell River* **2020**, *42*, 7.

49. Mewded, M.; Abebe, A.; Tilahun, S.; Agide, Z. Impact of land use and land cover change on the magnitude of surface runoff in the endorheic Hayk Lake basin, Ethiopia. *SN Appl. Sci.* **2021**, *3*, 742. [CrossRef]